3D sparse representations on the sphere
Applications in astronomy
Wavelets and Sparsity XV

François Lanusse, Jean-Luc Starck

CosmoStat Laboratory
Laboratoire AIM, UMR CEA-CNRS-Paris 7, Irfu, SAp, CEA-Saclay

August 27, 2013

Introduction

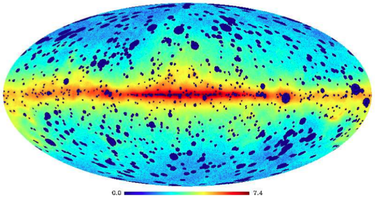

Simulated Fermi data denoised and inpainted by MS−VSTS+IUWT

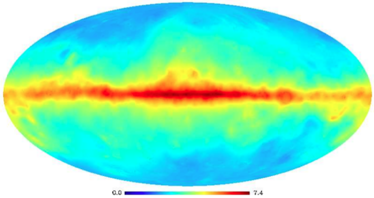

- Multiresolution transforms on the sphere have been very successful in a number of applications:
    - Denoising
    - Deconvolution
    - Component separation
    - Inpainting
- Can we extend these transforms to 3D signals on the Sphere ?

Introduction

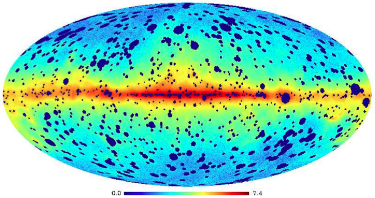

Simulated Fermi data denoised and inpainted by MS−VSTS+IUWT

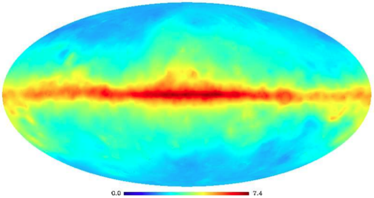

- Multiresolution transforms on the sphere have been very successful in a number of applications:
  - Denoising
  - Deconvolution
  - Component separation
  - Inpainting
- Can we extend these transforms to 3D signals on the Sphere ?

Introduction

We disitinguish 2 types of 3D signals:

Introduction

We disitinguish 2 types of 3D signals:

- **2D-1D**: 3rd dimension separable from the angular domain.
  Additional dependency can be in:
  - Time
  - Energy

Simulated Gamma-Ray Sky observed by the Fermi Space Telescope. Credit: NASA

Introduction

We disitinguish 2 types of 3D signals:

- **2D-1D**: 3rd dimension separable from the angular domain.
  Additional dependency can be in:
  - Time
  - Energy

Simulated Gamma-Ray Sky observed by the Fermi Space Telescope. Credit: NASA

- **3D**: 3rd dimension is the radial distance.
  These are signals on the 3D ball.

2 Micron All-Sky Redshift Survey. Credit: T. Jarrett (IPAC/Caltech)

Layout

1. 2D-1D sparse representation
   - Formulation of the 2D-1D wavelet
   - 2D-1D spherical undecimated wavelet
   - Application: Multichannel Deconvolution

2. 3D wavelet on the ball
   - The Spherical Fourier-Bessel Transform
   - IUWT in the SFB framework
   - Toy Experiment: Wavelet Denoising

Formulation of the 2D-1D wavelet

- The 2D and 1D dimensions do not have the same physical meaning $\Longrightarrow$ **Time or energy scales should not be connected to spatial scales.**

- The 2D-1D wavelet function is built by tensor product of a 2D spherical wavelet and a 1D wavelet:

$$\psi(\theta, \varphi, t) = \psi^{(\theta,\phi)}(\theta, \varphi)\psi^{(t)}(t)$$

- Any choice of wavelets can be used.

- Here, we consider only **dyadic scales** and **isotropic angular scales**.
- We use a 2D Isotropic Undecimated Wavelet Transform on the Sphere (Starck et al. 2006) and a 1D Starlet transform (Starck et al. 2009).
- For both transforms, wavelet coefficients are defined as the difference of 2 approximations:

$$w_{j+1} = c_j - c_{j+1} \tag{1}$$

Formulation of the 2D-1D wavelet

- The 2D and 1D dimensions do not have the same physical meaning $\Longrightarrow$ **Time or energy scales should not be connected to spatial scales.**
- The 2D-1D wavelet function is built by tensor product of a 2D spherical wavelet and a 1D wavelet:

$$\psi(\theta, \varphi, t) = \psi^{(\theta,\phi)}(\theta, \varphi)\psi^{(t)}(t)$$

- Any choice of wavelets can be used.
- Here, we consider only **dyadic scales** and **isotropic angular scales**.
- We use a 2D Isotropic Undecimated Wavelet Transform on the Sphere (Starck et al. 2006) and a 1D Starlet transform (Starck et al. 2009).
- For both transforms, wavelet coefficients are defined as the difference of 2 approximations:

$$w_{j+1} = c_j - c_{j+1} \tag{1}$$

Formulation of the 2D-1D wavelet

- The 2D and 1D dimensions do not have the same physical meaning $\Longrightarrow$ **Time or energy scales should not be connected to spatial scales.**
- The 2D-1D wavelet function is built by tensor product of a 2D spherical wavelet and a 1D wavelet:

$$\psi(\theta, \varphi, t) = \psi^{(\theta,\phi)}(\theta, \varphi)\psi^{(t)}(t)$$

- Any choice of wavelets can be used.
- Here, we consider only **dyadic scales** and **isotropic angular scales**.
- We use a 2D Isotropic Undecimated Wavelet Transform on the Sphere (Starck et al. 2006) and a 1D Starlet transform (Starck et al. 2009).
- For both transforms, wavelet coefficients are defined as the difference of 2 approximations:

$$w_{j+1} = c_j - c_{j+1} \tag{1}$$

2D-1D spherical undecimated wavelet

We consider a discrete signal $D[k_\theta, k_\varphi, k_t]$, J_1 angular scales and J_2 time/energy scales.

- Apply 2D spherical wavelet transform on each time frame $D[\cdot, \cdot, k_t]$:

$$D[\cdot, \cdot, k_t] = c_{J_1}[\cdot, \cdot, k_t] + \sum_{j_1=1}^{J1} w_{j_1}[\cdot, \cdot, k_t]$$

- Apply a 1D wavelet on all 2D wavelet scales $w_{j_1}[k_\theta, k_\varphi, \cdot]$ and approximation $c_{J_1}[k_\theta, k_\varphi, \cdot]$:

$$w_{j_1}[k_\theta, k_\varphi, \cdot] = w_{j_1, J_2}[k_\theta, k_\varphi, \cdot] + \sum_{j_2=1}^{J_2} w_{j_1, j_2}[k_\theta, k_\varphi, \cdot]$$

$$c_{J_1}[k_\theta, k_\varphi, \cdot] = c_{J_1, J_2}[k_\theta, k_\varphi, \cdot] + \sum_{j_2=1}^{J_2} w_{J_1, j_2}[k_\theta, k_\varphi, \cdot]$$

2D-1D spherical undecimated wavelet

We consider a discrete signal $D[k_\theta, k_\varphi, k_t]$, J_1 angular scales and J_2 time/energy scales.

- Apply 2D spherical wavelet transform on each time frame $D[\cdot, \cdot, k_t]$:

$$D[\cdot, \cdot, k_t] = c_{J_1}[\cdot, \cdot, k_t] + \sum_{j_1=1}^{J1} w_{j_1}[\cdot, \cdot, k_t]$$

- Apply a 1D wavelet on all 2D wavelet scales $w_{j_1}[k_\theta, k_\varphi, \cdot]$ and approximation $c_{J_1}[k_\theta, k_\varphi, \cdot]$:

$$w_{j_1}[k_\theta, k_\varphi, \cdot] = w_{j_1, J_2}[k_\theta, k_\varphi, \cdot] + \sum_{j_2=1}^{J_2} w_{j_1, j_2}[k_\theta, k_\varphi, \cdot]$$

$$c_{J_1}[k_\theta, k_\varphi, \cdot] = c_{J_1, J_2}[k_\theta, k_\varphi, \cdot] + \sum_{j_2=1}^{J_2} w_{J_1, j_2}[k_\theta, k_\varphi, \cdot]$$

2D-1D spherical undecimated wavelet

2D-1D spherical undecimated wavelet representation of D:

$$D[k_\theta, k_\varphi, k_t] = \underbrace{c_{J_1,J_2}[k_\theta, k_\varphi, k_t]}_{\text{2D approximation-1D approximation}} + \sum_{j_1=1}^{J_1} \underbrace{w_{j_1,J_2}[k_\theta, k_\varphi, k_t]}_{\text{2D detail-1D approximation}}$$

$$+ \sum_{j_2=1}^{J_2} \underbrace{w_{J_1,j_2}[k_\theta, k_\varphi, k_t]}_{\text{2D approximation-1D detail}} + \sum_{j_1=1}^{J_1} \sum_{j_2=1}^{J_2} \underbrace{w_{j_1,j_2}[k_\theta, k_\varphi, k_t]}_{\text{2D detail-1D detail}}$$

Applications:

- Transient source detection.
- Poisson denoising.
- Multichannel deconvolution.

Application: Multichannel Deconvolution

LAT instrument on the Fermi Space Telescope

- Observes the gamma-ray sky between 20 MeV-300 GeV.
- Energy dependent PSF.
- Poisson noise from very low fluxes.

Application: Multichannel Deconvolution

LAT instrument on the Fermi Space Telescope

- Observes the gamma-ray sky between 20 MeV-300 GeV.
- Energy dependent PSF.
- Poisson noise from very low fluxes.

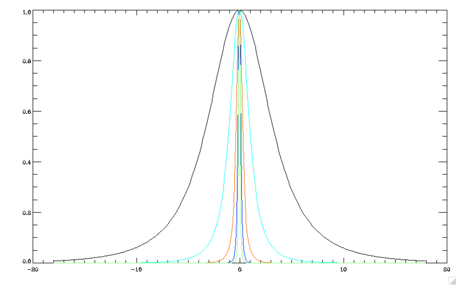

Figure : Normalized profile of the PSF for different energy bands.

Application: Multichannel Deconvolution

LAT instrument on the Fermi Space Telescope

- Observes the gamma-ray sky between 20 MeV-300 GeV.
- Energy dependent PSF.
- Poisson noise from very low fluxes.

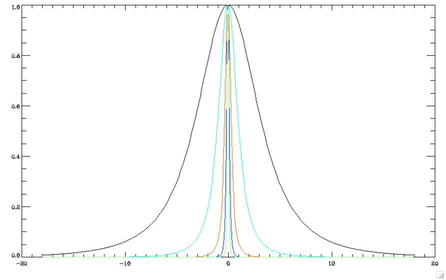

Figure : Normalized profile of the PSF for different energy bands.

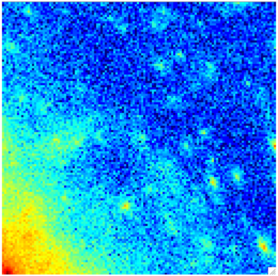

Figure : Simulated Fermi data between 220 MeV and 360 MeV.

Deconvolution technique

Approach developed in J. Schmitt et al. (2012): **Multichannel MS-VSTS** + modified **Richardson-Lucy** algorithm.

- Variance stabilization of a filtered signal (Zhang et al. 2008):

$$\mathcal{A}_j(c_j) = b^{(j)} \mathrm{sign}(c_j + \tau^{(j)}) \sqrt{|c_j + \tau^{(j)}|}$$

  $b^{(j)}$ and $\tau^{(j)}$ only depend on the filter, independent of the signal.

- Stabilized 2D-1D wavelet coefficients are obtained as the difference between 2 stabilized approximations.
- A **multiresolution support** $\mathcal{M}$ is built from significant stabilized wavelet coefficients.
- Deconvolution using a modified **Richardson-Lucy** algorithm with an additional sparsity regularization constraint from the multiresolution support $\mathcal{M}$.

Deconvolution technique

Approach developed in J. Schmitt et al. (2012): **Multichannel MS-VSTS** + modified **Richardson-Lucy** algorithm.

- Variance stabilization of a filtered signal (Zhang et al. 2008):

$$\mathcal{A}_j(c_j) = b^{(j)}\mathrm{sign}(c_j + \tau^{(j)})\sqrt{|c_j + \tau^{(j)}|}$$

  $b^{(j)}$ and $\tau^{(j)}$ only depend on the filter, independent of the signal.

- Stabilized 2D-1D wavelet coefficients are obtained as the difference between 2 stabilized approximations.

- A **multiresolution support** $\mathcal{M}$ is built from significant stabilized wavelet coefficients.

- Deconvolution using a modified **Richardson-Lucy** algorithm with an additional sparsity regularization constraint from the multiresolution support $\mathcal{M}$.

Deconvolution technique

Approach developed in J. Schmitt et al. (2012): **Multichannel MS-VSTS** + modified **Richardson-Lucy** algorithm.

- Variance stabilization of a filtered signal (Zhang et al. 2008):

$$\mathcal{A}_j(c_j) = b^{(j)}\mathrm{sign}(c_j + \tau^{(j)})\sqrt{|c_j + \tau^{(j)}|}$$

  $b^{(j)}$ and $\tau^{(j)}$ only depend on the filter, independent of the signal.

- Stabilized 2D-1D wavelet coefficients are obtained as the difference between 2 stabilized approximations.

- A **multiresolution support** $\mathcal{M}$ is built from significant stabilized wavelet coefficients.

- Deconvolution using a modified **Richardson-Lucy** algorithm with an additional sparsity regularization constraint from the multiresolution support $\mathcal{M}$.

Deconvolution technique

Approach developed in J. Schmitt et al. (2012): **Multichannel MS-VSTS** + modified **Richardson-Lucy** algorithm.

- Variance stabilization of a filtered signal (Zhang et al. 2008):

$$\mathcal{A}_j(c_j) = b^{(j)}\mathrm{sign}(c_j + \tau^{(j)})\sqrt{|c_j + \tau^{(j)}|}$$

  $b^{(j)}$ and $\tau^{(j)}$ only depend on the filter, independent of the signal.

- Stabilized 2D-1D wavelet coefficients are obtained as the difference between 2 stabilized approximations.

- A **multiresolution support** $\mathcal{M}$ is built from significant stabilized wavelet coefficients.

- Deconvolution using a modified **Richardson-Lucy** algorithm with an additional sparsity regularization constraint from the multiresolution support $\mathcal{M}$.

Deconvolution technique

Approach developed in J. Schmitt et al. (2012): **Multichannel MS-VSTS** + modified **Richardson-Lucy** algorithm.

- Variance stabilization of a filtered signal (Zhang et al. 2008):

$$\mathcal{A}_j(c_j) = b^{(j)}\mathrm{sign}(c_j + \tau^{(j)})\sqrt{|c_j + \tau^{(j)}|}$$

  $b^{(j)}$ and $\tau^{(j)}$ only depend on the filter, independent of the signal.

- Stabilized 2D-1D wavelet coefficients are obtained as the difference between 2 stabilized approximations.

- A **multiresolution support** $\mathcal{M}$ is built from significant stabilized wavelet coefficients.

- Deconvolution using a modified **Richardson-Lucy** algorithm with an additional sparsity regularization constraint from the multiresolution support $\mathcal{M}$.

Results

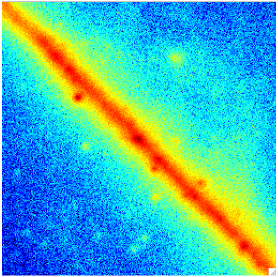

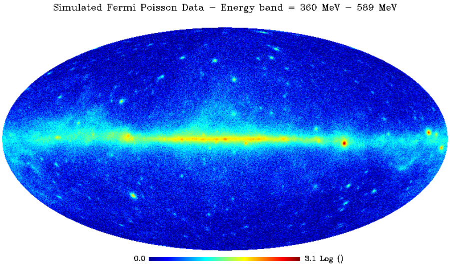
Simulated Fermi Poisson Data – Energy band = 360 MeV – 589 MeV
0.0
3.1 Log ()

Results

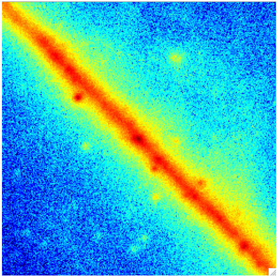

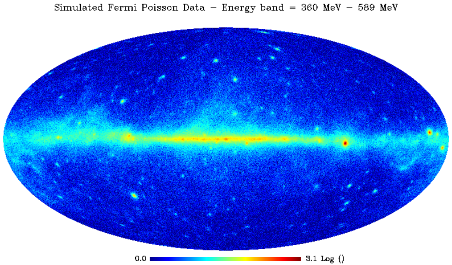
Simulated Fermi Poisson Data – Energy band = 360 MeV – 589 MeV
0.0
3.1 Log ()

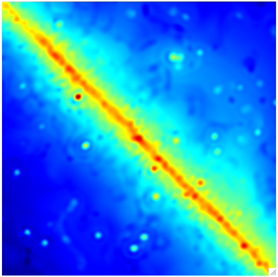

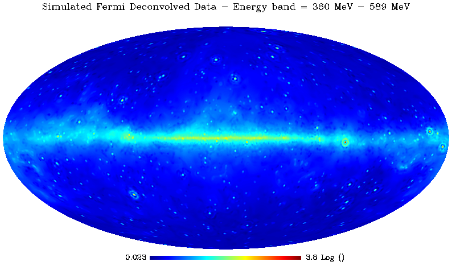
Simulated Fermi Deconvolved Data – Energy band = 360 MeV – 589 MeV
0.023
3.8 Log ()

Layout

Signals expressed on the 3D ball

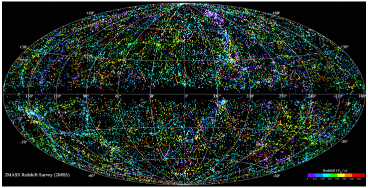

- Galaxy surveys aim at studying the matter density field in the universe.
  $\Longrightarrow$ 3D field observed in spherical coordinates (r, θ, φ).
- The specific physical meaning of the radial distance must be taken into account.
- Angular and radial domain are no longer completely separable.

Signals expressed on the 3D ball

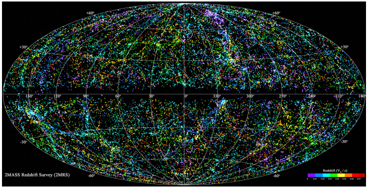

- Galaxy surveys aim at studying the matter density field in the universe. $\Longrightarrow$ 3D field observed in spherical coordinates (r, θ, φ).
- The specific physical meaning of the radial distance must be taken into account.
- Angular and radial domain are no longer completely separable.

Signals expressed on the 3D ball

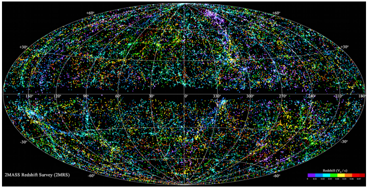

- Galaxy surveys aim at studying the matter density field in the universe.
  $\Longrightarrow$ 3D field observed in spherical coordinates (r, θ, φ).
- The specific physical meaning of the radial distance must be taken into account.
- Angular and radial domain are no longer completely separable.

Our approach

3D wavelet on the ball based on the **natural harmonic expansion** in spherical coordinates: the **Spherical Fourier-Bessel** Transform.

The Spherical Fourier-Bessel Transform

The Spherical Fourier-Bessel Transform of f is its development onto the following orthogonal basis:

$$\Psi_{lmk}(r,\theta,\phi) = \sqrt{\frac{2}{\pi}} j_l(kr) Y_l^m(\theta,\phi)$$

Spherical Fourier-Bessel Transform

Direct Transform:

$$\hat{f}_{lm}(k) = \sqrt{\frac{2}{\pi}} \int_\Omega \int f(r,\theta,\phi) \underbrace{r^2 j_l(kr) dr}_{\text{Spherical Bessel}} \underbrace{\overline{Y_l^m}(\theta,\phi) d\Omega}_{\text{Spherical Harmonics}}$$

Inverse Transform:

$$f(r,\theta,\phi) = \sqrt{\frac{2}{\pi}} \sum_{l=0}^{\infty} \sum_{m=-l}^{l} \int \hat{f}_{lm}(k) k^2 j_l(kr) dk Y_l^m(\theta,\phi) \quad (2)$$

IUWT in the SFB framework

All we need is to be able to express the convolution of f with a scaling function as a function of Spherical Fourier Bessel coefficients.

IUWT in the SFB framework

All we need is to be able to express the convolution of f with a scaling function as a function of Spherical Fourier Bessel coefficients.

Isotropic Low-Pass filtering in SFB

Scaling function $\phi^{k_c}(r, \theta_r, \phi_r)$ with cut-off k_c and spherical symmetry:

- $\hat{\phi}^{k_c}_{lm}(k) = 0$ as soon as $(l, m) \neq (0, 0)$
  $\hat{\phi}^{k_c}_{00}(k) = 0$ for all $k \geq k_c$
- $\boxed{\widehat{(f * \phi)}_{lm}(k) = \sqrt{2}\pi \hat{\phi}_{00}(k) \hat{f}_{lm}(k)}$

$\Longrightarrow$ Applying a 3D isotropic low-pass filter is equivalent to **multiplying** the SFB coefficients by a **function of k only**.

IUWT in the SFB framework

- $c^j(r, \theta_r, \phi_r)$ are a sequence of smooth approximations of $f(r, \theta_r, \phi_r)$
- c^j are expressed as the convolution of $f(r, \theta_r, \phi_r)$ with $\phi^{2^{-j}k_c}$:

$$\begin{aligned} c^0 &= \Phi^{k_c} * f \\ c^1 &= \Phi^{2^{-1}k_c} * f \\ &\dots \\ c^j &= \Phi^{2^{-j}k_c} * f \end{aligned}$$

- Wavelet coefficients are the difference between two successive smoothed approximations:

$$w^{j+1}(r, \theta_r, \phi_r) = c^j(r, \theta, \phi) - c^{j+1}(r, \theta, \phi)$$

IUWT in the SFB framework

Recursive definition of the wavelet decomposition

If $\hat{c}^0_{lm}(k) = \hat{f}_{lm}(k)$ then:

$$\begin{aligned} \hat{c}^{j+1}_{lm}(k) &= \hat{h}^j_{00}(k)\hat{c}^j_{lm}(k) \\ \hat{w}^{j+1}_{lm}(k) &= \hat{g}^j_{00}(k)\hat{c}^j_{lm}(k) \end{aligned}$$

Spherical Fourier-Bessel coefficients of the Wavelet decomposition:

$$\left\{\hat{w}^1, \hat{w}^2, \dots, \hat{w}^{J-1}, \hat{c}^J\right\}$$

with $\boxed{\hat{h}^j_{00}(k) = \frac{\hat{\Phi}^{2^{-(j+1)}k_c}_{00}(k)}{\hat{\Phi}^{2^{-(j)}k_c}_{00}(k)}}$ and $\boxed{\hat{h}^j_{00}(k) = 1 - \frac{\hat{\Phi}^{2^{-(j+1)}k_c}_{00}(k)}{\hat{\Phi}^{2^{-j}k_c}_{00}(k)}}$

IUWT in the SFB framework

Recursive definition of the filtered wavelet reconstruction

Given $\left\{\hat{w}^1, \hat{w}^2, \ldots, \hat{w}^{J-1}, \hat{c}^J\right\}$:

$$\hat{c}^j_{lm}(k) = \hat{c}^{j+1}_{lm}(k)\hat{\tilde{h}}^j_{lm}(k) + \hat{w}^{j+1}_{lm}\hat{\tilde{g}}^j_{lm}(k)$$

which yields $\hat{c}^0_{lm}(k) = \hat{f}_{lm}(k)$.

where $\hat{\tilde{h}}^j$ and $\hat{\tilde{g}}^j$ are defined as:

$$\begin{aligned}
\hat{\tilde{h}}^j_{lm}(k) &= \frac{\overline{\hat{h}^j}_{lm}(k)}{|\hat{h}^j_{lm}(k)|^2 + |\hat{g}^j_{lm}(k)|^2} \\
\hat{\tilde{g}}^j_{lm}(k) &= \frac{\overline{\hat{g}^j}_{lm}(k)}{|\hat{h}^j_{lm}(k)|^2 + |\hat{g}^j_{lm}(k)|^2}
\end{aligned}$$

IUWT in the SFB framework

Choice of the scaling function

Any scaling function verifying the spherical symmetry and cutoff frequency will do.
We use a 3rd order B-Spline for its good behavior in direct space.

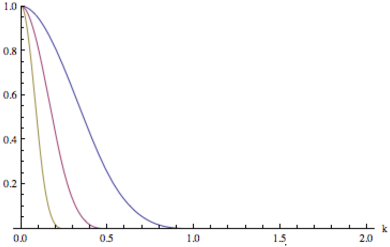

(a) Scaling function $\hat{\Phi}_{00}^{2^{-j}k_c}(k)$ for $j = 0, 1, 2$

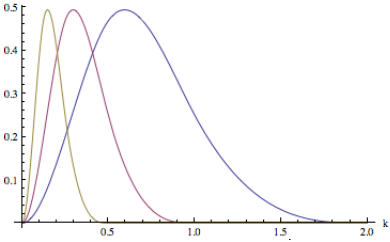

(b) Wavelet function $\hat{\Psi}_{00}^{2^{-j}k_c}(k)$ for $j = 0, 1, 2$

Spherical 3D Isotropic Undecimated Wavelet

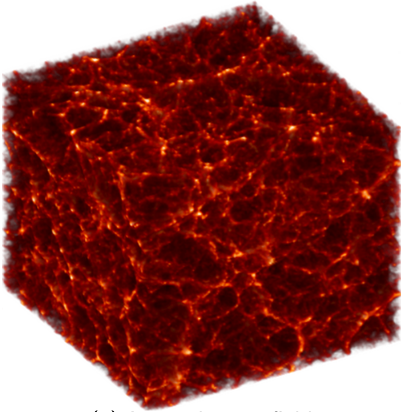

(c) Input density field

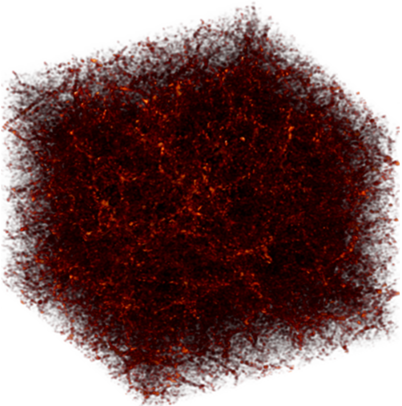

(d) First wavelet scale

Spherical 3D Isotropic Undecimated Wavelet

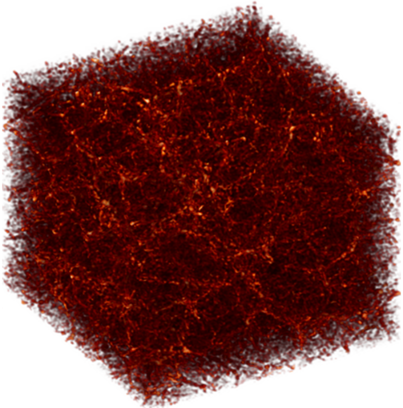

(e) Second wavelet scale

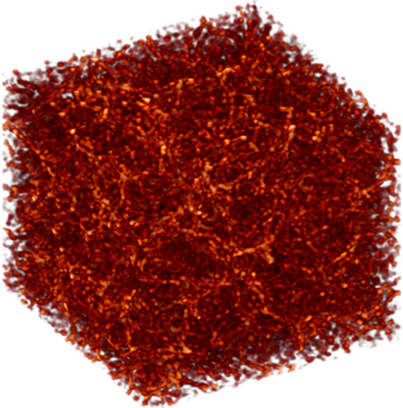

(f) Third wavelet scale

Spherical 3D Isotropic Undecimated Wavelet

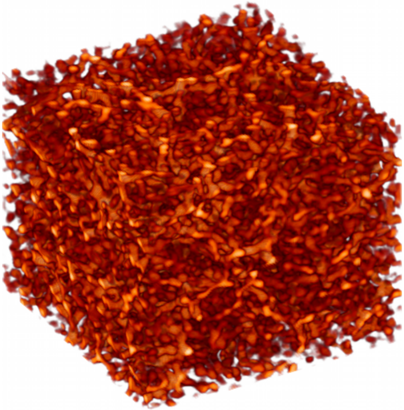

(g) Fourth wavelet scale

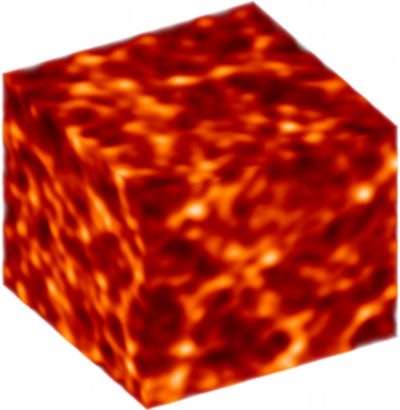

(h) Smoothed density

Practical implementation

Practical difficulties

- This only gives a continuous definition of the wavelet transform.
- A lot of algorithms are iterative and require back and forth wavelet transforms.

$\Longrightarrow$ In practice you need a **discrete sampling scheme** of (r, θ, ϕ) AND (l, m, k) which allows for **back and forth SFB transform**.
However there is no exact quadrature formula for the radial Spherical Bessel transform.

Luckily 2 things happen:

- **HEALPix angular discretization scheme** allowing for fast SHT transform in the SFB transform as demonstrated in **Leistedt et al. (2012)**
- When assuming **boundary conditions on the field**, the Spherical Bessel Transform can be **approximated** by **discrete** transform.

Practical implementation

Practical difficulties

- This only gives a continuous definition of the wavelet transform.
- A lot of algorithms are iterative and require back and forth wavelet transforms.

$\Longrightarrow$ In practice you need a **discrete sampling scheme** of (r, θ, ϕ) AND (l, m, k) which allows for **back and forth SFB transform**.
However there is no exact quadrature formula for the radial Spherical Bessel transform.

Luckily 2 things happen:

- **HEALPix angular discretization scheme** allowing for fast SHT transform in the SFB transform as demonstrated in **Leistedt et al. (2012)**
- When assuming **boundary conditions on the field**, the Spherical Bessel Transform can be **approximated** by **discrete** transform.

The Discrete Spherical Fourier Bessel Transform

The 2 ingredients of the DSFBT:

- **Angular transform** : HEALpix grid
- **Radial transform** : Discrete Spherical Bessel grid in k and r

Approximated transform

The transform is not exact **BUT** can be evaluated at any desired accuracy by increasing the number of points in the radial sampling.

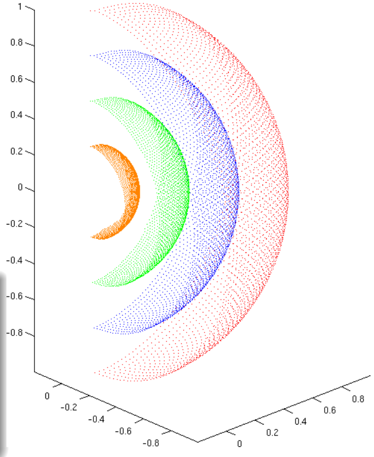

Figure : Spherical 3D grid

$$\boxed{f(r_{l_0 n}, \theta_{pix}, \phi_{pix}) \Longleftrightarrow \hat{f}(l, m, k_{ln})}$$

Toy Experiment: Denoising by hard thresholding

We extracted a density field from an Nbody simulation, added gaussian noise and expanded the field in Spherical Fourier-Bessel Coefficients.

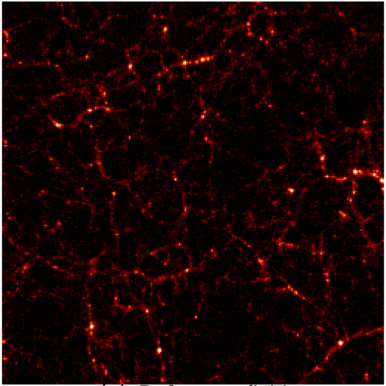

(a) Reference field

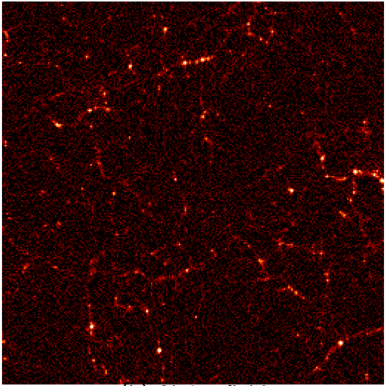

(b) Noisy field

Figure : Slice in the reconstruction of the test density field from the original and noisy Spherical Fourier-Bessel coefficients

Toy Experiment: Denoising by hard thresholding

Hard thresholding on the wavelet coefficients is done by setting to zero on each wavelet scale the coefficients below a given $\sigma_T = k\sigma_N$.

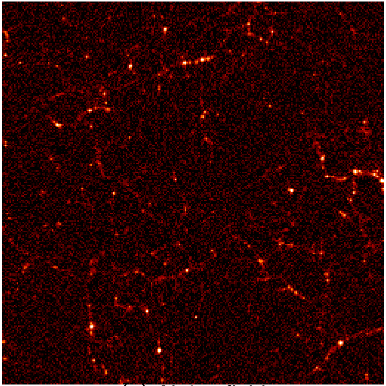

(a) Noisy field

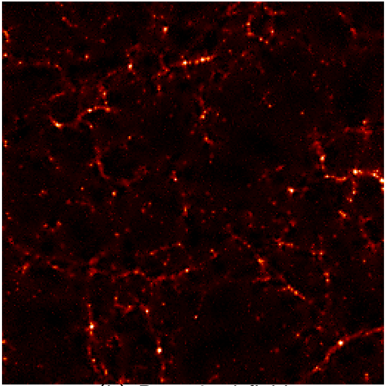

(b) De-noised field

Figure : Slice in the reconstruction of the noisy and de-noised Spherical Fourier-Bessel coefficients

Conclusion

We have presented 2 kinds of sparse representations on the sphere

- 2D-1D representations which can extend existing transforms on the sphere to 3D signals
- 3D isotropic wavelets on the ball

Such sparse representations can be used in many data restoration applications.

Codes for the 2D-1D transform: **http://jstarck.free.fr/isap.html**

All the codes for computing 3D wavelets is contained in a parallelized C++ package with an IDL interface: **http://jstarck.free.fr/mrs3d.html**

3DEX: Fast Spherical Fourier-Bessel decomposition of 3D surveys, Leistedt et al. (2012): **https://github.com/ixkael/3DEX**